Granule Lattice Protein 1 (Grl1p), an Acidic, Calcium-binding Protein in *Tetrahymena thermophila* Dense-Core Secretory Granules, Influences Granule Size, Shape, Content Organization, and Release but Not Protein Sorting or Condensation

N. Doane Chilcoat, Sharon M. Melia, Alex Haddad, and Aaron P. Turkewitz

Department of Molecular Genetics and Cell Biology, The University of Chicago, Chicago, Illinois 60637

Abstract. The electron-dense cores of regulated secretory granules in the ciliate *Tetrahymena thermophila* are crystal lattices composed of multiple proteins. Granule synthesis involves a series of steps beginning with protein sorting, followed by the condensation and precise geometric assembly of the granule cargo. These steps may to various degrees be determined by the cargo proteins themselves. A prominent group of granule proteins, in ciliates as well as in vertebrate neuronal and endocrine cells, are acidic, heat-stable, and bind calcium. We focused on a protein with these characteristics named granule lattice protein 1 (Grl1p), which represents 16% of total granule contents, and we have now cloned the corresponding gene. Mutants in which the macronuclear copies of *GRL1* have been disrupted continue to synthesize dense-core granules but are nonetheless defective in regulated protein secretion. To understand the nature of this defect, we characterized mutant and wild-type granules. In the absence of Grl1p, the sorting of the remaining granule proteins appears normal, and they condense to form a well-defined core. However, the condensed cores do not demonstrate a visible crystalline lattice, and are notably different from wild type in size and shape. The cellular secretion defect arises from failure of the aberrant granule cores to undergo rapid expansion and extrusion after exocytic fusion of the granule and plasma membranes. The results suggest that sorting, condensation, and precise granule assembly are distinct in their requirements for Grl1p.

DENSE-CORE granules are cytoplasmic storage vesicles for condensed secretory proteins (69). Their fusion with the plasma membrane with consequent secretion of the granule contents is triggered by extracellular stimuli (3, 16). This pathway has been most thoroughly described in vertebrate endocrine, exocrine, and neuronal cells, in which studies based chiefly on biochemical and cell biological approaches have demonstrated differences from the pathway of constitutive protein secretion at numerous steps (57). First, granule contents are efficiently sorted from other proteins in the secretory pathway (15, 48). A possible mechanism for sorting was initially proposed based on the appearance of large protein aggregates within the TGN of regulated secretory cells (29, 61, 85). Their formation suggested that granule proteins could coaggregate and thus segregate from other soluble proteins in transit. Neither the aggregate organization nor the molecular determinants that drive aggregation is understood. Various granule proteins show a tendency to aggregate in vitro under conditions believed to exist in the TGN (19, 38, 40, 46, 76, 90), namely mild acidity and high calcium (4, 20). In some cases, the aggregation of specific proteins is enhanced in the presence of others, leading to suggestions that specific coaggregation might be an important mechanism for sorting heterologous components to a developing granule (24, 39, 40). However, it should be noted that the physiological relevance of in vitro aggregation has been difficult to confirm. For example, the disruption of calcium gradients by ionophores did not interfere with granule protein sorting in a permeabilized cell system (17).

Granule protein aggregates are incorporated into vesicles budding from the TGN. The fusion of several such vesicles may form the initial immature dense-core granule, which subsequently undergoes a maturation process characterized by visible protein condensation and proteolytic processing (71, 82, 84, 85). This process is well illustrated by insulin storage granules. Insulin is synthesized and transported to the TGN as a prohormone (28, 60, 61). During granule formation, proinsulin is cleaved by at least

Address all correspondence to Aaron Turkewitz, MGCB, University of Chicago, 920 E. 58th Street, Chicago, IL 60637. Tel.: (773) 702-4374. Fax: (773) 702-3172. E-mail: apturkew@midway.uchicago.edu

two enzymes in the prohormone convertase family (26, 79). The convertase activities are themselves regulated by proton and calcium concentrations, both of which increase during granule maturation (26, 62). The mature insulin product crystallizes to form a dense core. Crystals are compact and allow storage of macromolecules in an osmotically inactive state. They are also formed in some granules containing several distinct proteins (83), including those in ciliates (43).

Unicellular systems offer an additional approach to studying this pathway: the ciliated protozoa *Tetrahymena* and *Paramecium*, which contain well-characterized secretory granules, have been particularly useful for genetic analysis. The steps leading to granule formation in ciliates and vertebrate endocrine cells appear similar, including appearance of protein aggregates (64), coalescence of TGN-derived vesicles to form the immature granules (44), and the proteolytic maturation of granule proproteins (2, 23, 27, 87). After maturation, ciliate granules dock at defined sites at the cell cortex. Extracellular stimulation leads to membrane fusion, and secretion itself takes the form of rapid expansion of the condensed crystalline cores, which are thereby ejected from the cells in the form of large ordered aggregates (42, 44, 54, 65). In these features, ciliate granules resemble cortical granules in oocytes that undergo fusion and expansion after fertilization (75).

In ciliates, mutants defective in regulated secretion can be identified by eye, since the large released aggregates are visible at the single cell level (66, 80). By using biochemical and morphological markers, such mutants have been assigned to distinct phenotypic classes: defects in granule formation and/or accumulation, aberrant granule morphology, defective transport and/or docking, or inefficient membrane fusion upon stimulation (6, 9, 11, 36, 41, 52, 63, 73, 86, 87). A limitation is that the genetic lesions responsible for these defects have not yet been identified; a single exception is the link between calmodulin mutations and exocytosis in *Paramecium* (49). In that case, mutations in calmodulin were initially characterized based on motility defects and later shown to affect regulated exocytosis.

Using *Tetrahymena thermophila*, in which the granules are known as mucocysts, one can now use recently developed methods for mass transformation, gene disruption and replacement to evaluate the roles of specific granule proteins in vivo (32, 34, 47). This paper addresses unresolved issues in granule synthesis and function by using a combination of two novel mutants. In the first of these, identified after chemical mutagenesis, granules fail to dock at the plasma membrane but instead accumulate in the cytoplasm. While the molecular defect is not known, it appears not to be in the granules per se but in a cytosolic factor. The second mutant is the result of targeted disruption of the gene encoding an abundant, 40-kD granule core protein, which was identified as an acidic, calcium-binding, heat-soluble species (87). Also of interest was the fact that the *Tetrahymena* protein, originally called p40, appeared to undergo proteolytic maturation in a step potentially involved in dense core formation. In this work, analysis of the individual and the double mutants allows us to investigate the roles of this core protein during protein sorting, granule maturation, and secretion.

Materials and Methods

All reagents were from Sigma Chemical Co. (St. Louis, MO) unless otherwise noted.

Cells and Cell Culture

Cells were grown at 30°C with agitation in 2% proteose peptone, 0.2% yeast extract (both from Difco Laboratories, Inc., Detroit, MI), with 0.003% ferric EDTA. *Tetrahymena* strains are designated by their micronuclear diploid genotype, followed by their macronuclear-determined phenotype in parentheses (14). The heterokaryon strain CU428.1, MPR^R/MPR^R(6-methylpurine–sensitive, VII) bears a dominant allele conferring 6-methylpurine resistance in the micronucleus and the corresponding sensitive allele in the macronucleus; strain B2086, mpr^S/mpr^S(6-methylpurine–sensitive, II) has the drug-sensitive allele in both nuclei. Both were kindly provided by Peter Bruns (Cornell University, Ithaca, NY) and are wild type with respect to exocytosis. The mutant strain MN173, MPR^R/MPR^R(6-methylpurine–resistant, V) was derived by Tim Soelter and Eric Cole (St. Olaf College, Northfield, MN), as a whole cell homozygote from strain CU428.1 after mutagenesis with nitrosoguanidine, using uniparental cytogamy (21). It was identified as exocytosis deficient because of its inability to produce visible pericellular capsules after stimulation with alcian blue; this assay has previously been used to identify a set of exocytosis mutants (12, 63, 80).

Nomenclature

Because no comprehensive genetic nomenclature for *Tetrahymena thermophila* has been uniformly adopted, this paper uses a nomenclature closely based on that used in *Saccharomyces cerevesiae* (77). *GRL1* refers to the wild-type gene; *GRL1::NEO2* designates the allele of that gene that has been disrupted by insertion of the *NEO2* allele. Dominant and recessive alleles are indicated in upper- and lowercase, respectively. Granule lattice protein 1 (Grl1p)[1] refers to the protein product of the wild-type gene.

Strain MN173 has not been genetically characterized and will be referred to in the text as doc$^-$ to indicate that its distinct phenotype is the accumulation of undocked granules, whereas the wild-type phenotype is Doc$^+$. *GRL1::NEO2* doc$^-$ designates disruption of the *GRL1* locus in the MN173 background.

Protein Purification and Sequencing

Secreted protein was purified from a 200-ml exponential culture of cells stimulated with dibucaine as previously described (87) but with the following changes: the buffer was 10 mM Tris, pH 7.0, 1 mM $CaCl_2$, and the protease inhibitors used were leupeptin (0.5 μg/ml), antipain (12.5 μg/ml), E-64 (10 μg/ml), and chymostatin (10 μg/ml). The purified protein was solubilized in SDS-containing sample buffer with 10 mM DTT at 65°C and fractionated by SDS-PAGE along with prestained molecular weight standards (BioRad Labs, Hercules, CA). After electrophoresis, the appropriate region of the gel was electrophoretically transfered to a polyvinylidene difluoride membrane (BioRad Labs) and then stained with Coomassie blue R-250. The strong band at ~40 kD was excised. NH_2-terminal sequencing was performed by the Protein Chemistry Laboratory, Washington University (St. Louis, MO). Protein concentrations were assayed using bicinchoninic acid (BCA) (Pierce, Rockford, IL). SDS-PAGE was performed according to Laemmli (51). Quantitation of Coomassie blue–stained gel bands was performed using a computing densitometer (Molecular Dynamics, Sunnyvale, CA).

Cloning of GRL1 cDNA and Genomic DNA

Based on known codon usage in *Tetrahymena thermophila* (55, with additional information provided by M. Gorovsky, University of Rochester, Rochester, NY), degenerate primers (Integrated DNA Technologies, Coralville, IA) were designed to amplify *GRL1* via the PCR. The 5′ primer 5′-GAATA (T/C)GT (T/C)AA (T/C)GC (T/C)GA (T/C)GA-3′ corresponded to amino acid residues 189–195 of the precursor protein; the

1. *Abbreviations used in this paper*: ECL, enhanced chemiluminescence; Grl1p, granule lattice protein 1; ORF, open reading frame; tmps, trichocyst matrix proteins.

3′ primer 5′-CC (A/G)ATTTC (A/G)TC (A/G)GC (A/G)GTTGC-3′ to residues 207–213. PCR was performed on a *Tetrahymena thermophila* λgt10 cDNA library generously provided by Tohru Takemasa (University of Tsukuba, Japan). The 50-μl reactions contained 10^8 plaque-forming units in ~5 μl SM buffer, 2.5 U Taq polymerase (Boehringer Mannheim Corp., Indianapolis, IN), 10 mM Tris-HCl, pH 8.3, 50 mM KCl, 2.5 mM $MgCl_2$, 250 nM each dNTP, and 1 mM each primer; 30 cycles of 94°C, 1 min; 50°C, 1 min; 72°C, 0.5 min were performed. This amplification produced a faint band of the expected size, 75 bp, which was subsequently amplified using 1 μl of the primary product as template. This product was cloned into pCRII (Invitrogen, San Diego, CA).

A single intron was suggested by Southern blotting of restriction digests of genomic and cDNA using ClaI and EcoNI. The site of the insertion was mapped to an 80-bp region between (or within) the degenerate 3′ primer and the EcoNI site. Using this information, primers were designed to border the intron: 5′ primer: 5′-ACTATTAATAACTCGCTCTCCTT-3′; 3′ primer: 5′-ATCCCTTTCTTTCACCTTCTT-3′. A fragment of the predicted size (718 bp) was amplified from total CU428.1 DNA (prepared as above, 10 ng/rxn) using the same conditions and program as above, and this product was subcloned into pCRII.

Genomic sequences 5′ of the cDNA were subcloned using inverse PCR (58) on genomic DNA digested with HindIII. The forward, 5′-CAGCAGCCAAAGCGAGGAA-3′, corresponded to bases 52–34 relative to the start codon, and the reverse primer 5′-ACCAACCAAAGTGAAGAAGAAG-3′ to bases 54–76. The PCR was performed on 200 ng of circularized genomic DNA using the same reagents and cycling times as above, but with 1.5 mM $MgCl_2$ and 1.5 min of extension. These reactions produced a single product, which was the expected size (1.2 kb) by Southern analysis. This was cloned into pCRII.

A genomic subclone of *GRL1* was obtained by amplifying total CU428.1 DNA (as above) using primers corresponding to the cDNA just 5′ of the poly-A tail (5′-AATGAATAGGAAAGAAAGAAAC-3′) and at the 5′ end of the upstream sequence (5′-TCCATTCACATAGAACATACAG-3′). An ~3 kb fragment was subcloned into pCRII as above, and the identity of the insert was confirmed by restriction analysis and partial sequencing.

The 75-bp PCR product was used to screen a cDNA phage library using standard techniques (72). A screen of 1.2×10^5 plaques identified 60 positives. 10 of these were analyzed and found to contain two insert classes of 1.2 and 1.5 kb, which had overlapping restriction maps. A 1.5-kb clone was cloned into pBluescript SK (+) (Stratagene, La Jolla, CA).

Southern and Northern Blotting Analysis

The 1.5-kb cDNA was purified from vector and labeled with digoxigenin (Boehringer Mannheim Corp.) by randomly primed DNA synthesis. Genomic DNA was prepared as described (33). Southern blotting was conducted using the Genius system (Boehringer Mannheim), loading ~10 μg of DNA per lane.

RNA purification was performed according to Cathala et al. (18) with the following modifications: Pelleted cells were lysed with 5 M guanidinium thiocyanate, 10 mM EDTA, 50 mM Tris-HCl, pH 7.5, 8 mM 2-mercaptoethanol. RNA was precipitated with 7 vol cold 4 M LiCl, and the pellet was washed once with 3 M LiCl and resuspended in 0.5% *N*-lauroylsarkosine, 1 mM EDTA, 10 mM Tris, pH 7.5. After phenol/chloroform extraction, RNA was ethanol precipitated, washed, and suspended in water. RNA electrophoresis and Northern blotting were performed as per Farrell (30). After electrophoresis on 1% agarose gels with formaldehyde, RNA was transfered and UV cross-linked to Magna (MSI, Westboro, MA) nylon membranes. Blots were hybridized in 5× SSPE, 5× Denhardt's, 50% formamide, 0.1% SDS, and 100 μg/ml denatured salmon sperm DNA, with 20 ng/ml probe concentration (~5×10^6 cpm/cm^2), and visualized using a Phosphorimager (Molecular Dynamics).

Mapping of RNA Ends

The precise 5′ end of the *GRL1* transcript was mapped using primer extension, as described in the Promega Technical Bulletin (Promega, Madison, WI). Briefly, a ^{32}P-labeled oligonucleotide primer corresponding to bases +15 through −11 (5′-TAATTTCTTATTCATTTGTCTGGATG-3′) was annealed to 15 μg total RNA at 60°C for 20 min. The reactions were allowed to cool to room temperature for 10 min, at which point RNA–primer complexes were extended with avian myoblastosis virus reverse transcriptase (Boehringer Mannheim) for 30–90 min at 42°C and then ethanol-precipitated and analyzed on a sequencing gel. Another primer corresponding to bases +52 through +33 (5′-CAGCAGCCAAAGCGAGGAA-3′) indicated the same 5′ termini. As a standard, sequencing using the same primers (but labeled with ^{33}P) was conducted on a cloned genomic copy of *GRL1*.

Sequencing and Sequence Analysis

The initial 75-bp PCR product and the cDNA clone were sequenced using M13 primers. The complete cDNA sequence was obtained by constructing deletion series using Exonuclease III and Mung Bean nuclease (72). Two deletion series, one from each end of the insert, were made so that both strands could be sequenced. The sequences of the intron and upstream region were obtained by primer walking. Sequencing was performed on plasmid or single-stranded DNA using the Applied Biosystems Taq Dyedeoxy Terminator Cycle Sequencing kit and an Applied Biosystems automated sequencer (Perkin Elmer, Foster City, CA) or the Sequenase v2.0 sequencing kit (United States Biochemical, Cleveland, OH) and a manual sequencing apparatus. The cDNA sequence was determined with at least twofold redundancy throughout the open reading frame (ORF) and 5′UTR on each strand. The 125 bases directly upstream of the poly-A tail were sequenced on one strand with at least twofold redundancy. Three independently amplified clones of the intron and upstream region were sequenced on both strands with at least twofold redundancy. Protein secondary structure was predicted using the Lasergene software package (DNAStar, Madison, WI). Alignment of the heptads between Grl1p and *Paramecium* proteins was done by eye.

Disruption of GRL1

GRL1 was disrupted by replacement of the sequences −15 to +260 relative to the start codon with a construct comprised of the *NEO* gene (which endows resistance to neomycin/paromomycin) under the control of the histone H4 promoter and β-tubulin 3′UTR (34), for which the name *NEO2* is proposed by J. Gaertig (University of Georgia, Athens, GA). Electroporation using the ECM 600 (BTX Inc., San Diego, CA) was conducted exactly as described on mating pairs of B2086 and CU428.1 (35). Initial drug selection was with 120 μg/ml paromomycin, added 6 h after transformation. Between 2 and 25 transformants were obtained per successful transformation. Because only some of the macronuclear *GRL1* copies are replaced initially, cells were cultured with increasing concentrations of paromomycin for stringent selection of the *GRL1::NEO2* allele. Several transformants were cloned and grown in increasing amounts of paromomycin (up to 1 mg/ml) for more than 80 generations. Three independent lines were analyzed further; they were phenotypically indistinguishable. Disruption of *GRL1* in vegetative doc$^-$ cells by the same construct was accomplished by biolistic transformation. Cells were starved overnight in 10 mM Tris, pH 7.5, and resuspended at 10^7 cells/ml in 10 mM Hepes, pH 7.5. Gold particle microprojectiles (1 μM, BioRad Labs) were prepared according to Sanford et al. (72a). Rupture membranes, macrocarrier flying disks, and wire-stopping screens (Rumsey Loomis Machine Shop, Ithaca, NY) with a Biolistic PDS-10000/He device (BioRad Labs) (Courtesy of J. Narita, University of Illinois, Chicago, IL) were used, at settings of 27–28 in Hg vacuum, 1/4 in gap distance, 8 mm macrocarrier travel, and a target distance of 9 cm, following an optimized protocol developed by Peter Bruns and colleagues (Cornell University, Ithaca, NY). Transformed cells were plated, and paromomycin was added to a final concentration of 120 μg/ml after 2 or 5 h. Resistant cells were isolated after 4 d. In two experiments, we obtained 527 and 685 transformants/shot.

Isolation of Dense-Core Granules

400–800 ml of *GRL1* doc$^-$ or *GRL1::NEO2* doc$^-$ cells were grown overnight to stationary phase and then rapidly chilled and pelleted at 150 *g* for 5 min in conical bottles. All subsequent operations were performed cold. Cells were washed once in 10 mM Hepes, pH 7.0, and the pellet volume measured. The pellet was then washed and resuspended in 2 vol of buffer A (0.3 M sucrose, 10 mM Hepes, pH 7, 28.8 mM KCl, 2 mM $MgCl_2$, 2 mM EGTA [Fluka Chemical Corp., Ronkonkoma, NY]) containing 0.1% gelatin and with protease inhibitors as above. The resuspended pellet was homogenized by passage through a ball bearing cell cracker (Hans Issel, Palo Alto, CA) with a nominal clearance of 0.0005 in. The homogenate was cleared for 10 min at 500 *g* and 5 ml of the supernatant was layered on a 20 ml pad of 60% Percoll (Pharmacia LKB Biotechnology, Piscataway, NJ) in buffer A with gelatin. These tubes were centrifuged for 15 min at 27,000 rpm (model Ti60; Beckman Instrs., Carlsbad, CA). Granules from *GRL1* doc$^-$ cells were harvested from a single distinct band near the tube bottom and were then diluted with buffer A without gelatin and pelleted

for 5 min at 5,000 *g*. Granules from *GRL1::NEO2* doc$^-$ cells also appeared as a distinct though less intense band at a similar position.

Granules were also partially resolved from other cell fractions using Nycodenz gradients (GIBCO BRL, Gaithersurg, MD). 0.4 ml of cleared lysates in buffer A, prepared as above, were applied to 9 ml continuous Nycodenz gradients (top solution: buffer A with additional 50 mM sucrose; bottom solution: 45% Nycodenz in buffer A) and centrifuged for 90 min at 120,000 *g*. 0.5 ml fractions were collected.

Electron Microscopy

All reagents were from EM Sciences (Ft. Washington, PA). Cells were fixed in 2% glutaraldehyde, 0.5% osmium tetroxide, 1.3 mM sodium phosphate, pH 7.0, 0.5% sucrose for 1 h at room temperature. To visualize protein secretion, cells were starved and stimulated with alcian blue as described above and fixed 3 s later. After partial dehydration, cells were stained for 1 h with 1% uranyl acetate in 70% ethanol. After dehydration through a graded series of ethanol solutions and polypropylene, samples were embedded in EMbed 812. Sections were stained with uranyl acetate and lead citrate and viewed using an electron microscope (model CX100; JEOL USA Inc., Peabody, MA). Purified granules were fixed overnight as pellets in 2% glutaraldehyde, 1% osmium tetroxide in buffer A, and processed as above. For negative staining, purified granules were adsorbed to carbon-coated grids and stained with 2% sodium phosphotungstate near pH 7.

Western Blotting and Immunofluorescence

The rabbit antisera specific for Grl1p and p80 and the mAb 4D11 against p80 have been previously described (86, 87). Antibody blotting was performed according to (87), and antibodies were visualized using the enhanced chemiluminescence (ECL) system (Amersham Corp., Arlington Heights, IL) and quantified using a computing densitometer (Molecular Dynamics). For immunofluorescence, cells were pelleted and fixed for 10 min in ice-cold 0.2% Triton X-100 in 50% ethanol. Blocking was for 30 min at room temperature in 0.5% BSA in Tris-buffered saline (0.9% NaCl in 20 mM Tris, pH 8.2), followed by pelleting and a 30-min incubation in 20% hybridoma supernatant in TBS. Cells were then washed three times for 5 min in BSA/TBS, followed by a 30-min incubation in 0.1% rhodamine isothiocyanate–coupled rabbit anti–mouse IgG (Calbiochem-Novabiochem, La Jolla, CA). They were then washed as before and resuspended in Slowfade (Molecular Probes, Eugene, OR), and confocal images were collected with a laser scanning microscope (model LSM 4; Carl Zeiss, Inc., Thornwood, NY), courtesy of Susan Lindquist (University of Chicago).

Results

Purification and Cloning of GRL1

We stimulated *Tetrahymena thermophila* to induce exocytosis of dense-core granules and purified the proteins released into the cell supernatant. From these we isolated by SDS-PAGE a 40-kD protein, focusing on it because we had previously noted its in vitro calcium-binding activity (87). It is probably identical to a 34-kD protein noted by Maihle and Satir (54) and is the single most abundant protein in dense-core granules, representing 16.0 ± 0.78% (n = 3) of the total protein based on densitometry of Coomassie-stained bands of SDS-PAGE–resolved proteins from purified granules (see Fig. 7 *A*, lane *1*). We propose the name granule lattice protein 1 (Grl1p) for this secreted protein.

To clone the corresponding gene, the first 26 residues of amino-terminal sequence were determined by Edman degradation to be EYVNADDYSVNPDYSTGDRTADEIGS. Degenerate primers were designed to amplify the corresponding sequence from a cDNA library. The PCR product was then used to screen a cDNA library. A clone was isolated and found to contain a 1.5-kb insert including a single ORF of 1,206 bp. Codon usage throughout the ORF was characteristic for *Tetrahymena thermophila*, including the use of TAA to encode glutamine (45, 55). The proposed ORF is flanked by AT-rich sequences, and the 3′ flank includes a sequence resembling a polyadenylation site (68) that is 73 bp downstream of the translation termination codon. Comparison with sequences obtained by amplification of genomic DNA revealed the presence of a single AT-rich 544-bp intron. The DNA and predicted amino acid sequences appear in Fig. 1.

Sequence Analysis

The sequence predicted by the ORF appeared to encode a precursor for Grl1p in the form of a pre-proprotein. The predicted polypeptide begins with a canonical signal sequence for translocation into the endoplasmic reticulum. Cleavage of this presequence was predicted to occur after alanine 18 (88). The ORF then extends for 1,152 nucleotides, yielding a translation product of 384–amino acid residues with a calculated mass of 43.4 kD. The NH_2-terminal

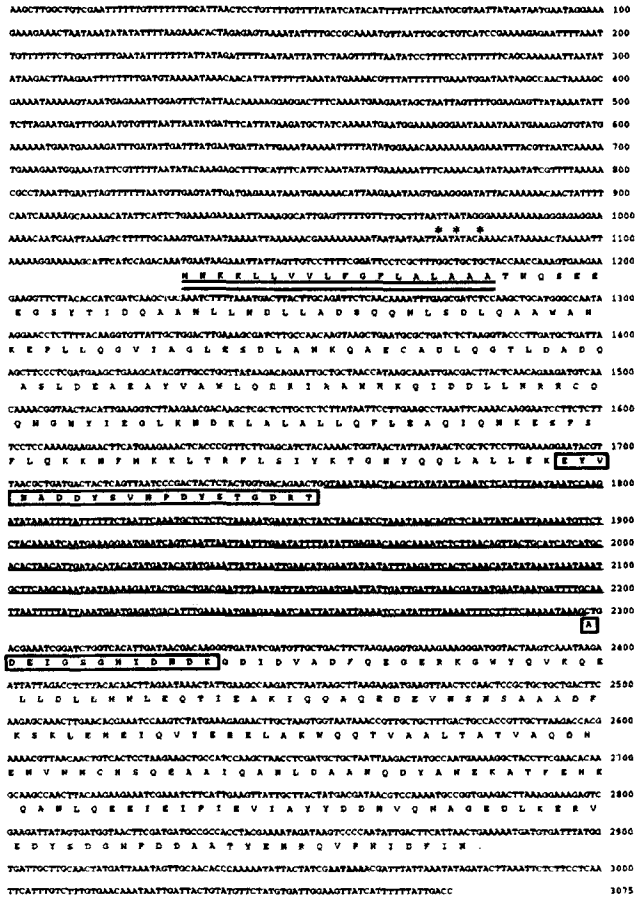

Figure 1. Sequence of *GRL1*. The deduced amino acid sequence is shown below the corresponding oligonucleotide sequence. Features have been indicated as follows: For the nucleotide sequence, the intron sequence is underlined, a putative polyadenylation site is emboldened, and the transcription start sites are marked by asterisks. For the protein, the peptide sequence (obtained by Edman degradation) that identifies the amino terminus of mature Grl1p is boxed; the predicted signal sequence is doubly underlined. These sequence data are available from GenBank/EMBL/DDB under accession number U72946.

peptide sequence obtained from the purified secreted protein appeared as an internal peptide beginning at glutamate 189, consistent with earlier evidence that the protein is derived proteolytically from a larger species (87). The calculated molecular mass of the mature protein is 24.3 kD. This was unexpected, since secreted Grl1p migrates as a 40-kD protein by SDS-PAGE. Similarly, although the precursor has a calculated size of 43.4 kD, it migrates as a 60-kD species by SDS-PAGE. In theory, these disparities may be due to posttranslational glycosylation; however, no indication of this was found by endoglycosidase treatment or sugar-specific labeling (not shown). Moreover, glycosylation of *Tetrahymena* granule proteins appears to be very limited (5). Instead, the high negative charge on the protein is likely to explain the anomalous migration during SDS-PAGE, a phenomenon also noted in some acidic vertebrate granule proteins (89). Acidic residues make up 23% of the Grl1p predicted sequence, leading to a predicted pI of 4.1 for the pro-protein and 4.0 for the mature protein. The pI of the mature protein has been estimated by isoelectric focusing at 4.0–4.2 (22); (Turkewitz, A.P., unpublished).

Structural predictions based on the translated sequence are shown in Fig. 2 *A*. Pre-pro-Grl1p has no extended hydrophobic stretches except that found in the NH_2-terminal presequence. Clusters of negatively charged residues are distributed throughout much of the protein, with notable exceptions in the signal sequence and two regions between amino acid residues 118–130 and 155–186. This second stretch contains a significant cluster of positively charged amino acids between residues 161–176. Interestingly, this cluster of single and paired basic residues is quite close to lysine 188, the site where proteolytic cleavage generates the mature protein. Most of the proprotein is predicted to adopt an α-helical conformation. Screening the protein data base for homologous sequences identified myosin family members and other proteins with coiled-coil domains (not shown). The homologies were confined to regions of Grl1p containing coil-forming heptads, as defined by the prevalence of apolar side chains at the *a* and *d* positions. Among these identified sequences was that of the T2-c protein present in the dense-core granule lattice of another ciliate, *Paramecium tetraurelia.* Granules in *Paramecium* are known as trichocysts, and T2-c is one of a family called trichynins, or trichocyst matrix proteins (tmps) (37, 78). Although the level of amino acid similarity between Grl1p and T2-c was low (<20%), the alignment of the Grl1p sequence with three tmps suggested significant structural similarity as indicated by the positions of the heptad motifs, particularly in the first half of the protein (Fig. 2 *B* and Discussion).

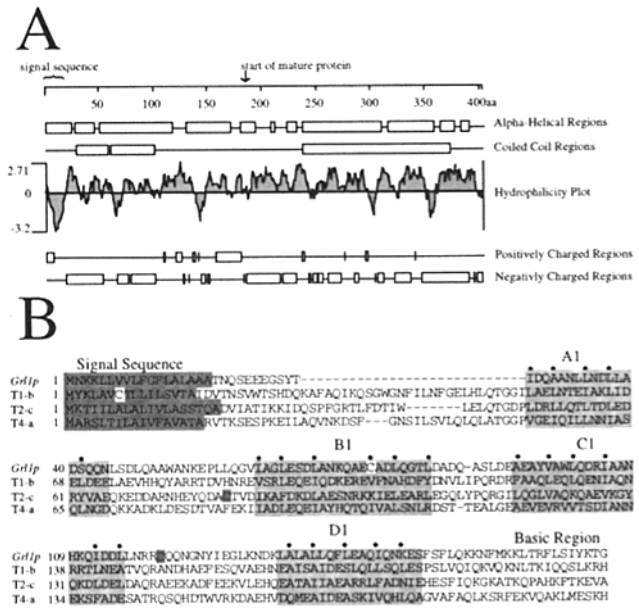

Figure 2. (*A*) The calculated translation product of the *GRL1* gene was analyzed for charge distribution and for predicted structural features. (*B*) Sequence comparison of amino-terminal regions of Grl1p and three *Paramecium* tmps. For Grl1p, the sequence shown corresponds to the proregion and ends 10 residues before the processing site that generates mature Grl1p. Predicted signal sequences are darkly shaded. Four regions containing heptad motifs predicted to form coiled-coils are lightly shaded, and the expected positions for hydrophobic residues are indicated by dots. The alignment of tmps, and the labeling of heptad regions as A1, B1, C1, and D1, is based on Gautier et al. (37). A region rich in basic residues is also indicated, although the boundaries are not identical for the four proteins. Cysteine residues have been shaded or, if they are located within shaded areas, lightened.

Gene Structure and Transcription

Northern blotting analysis of RNA indicated a single major mRNA transcript of 1.4 kb (Fig. 3 *A*). To determine

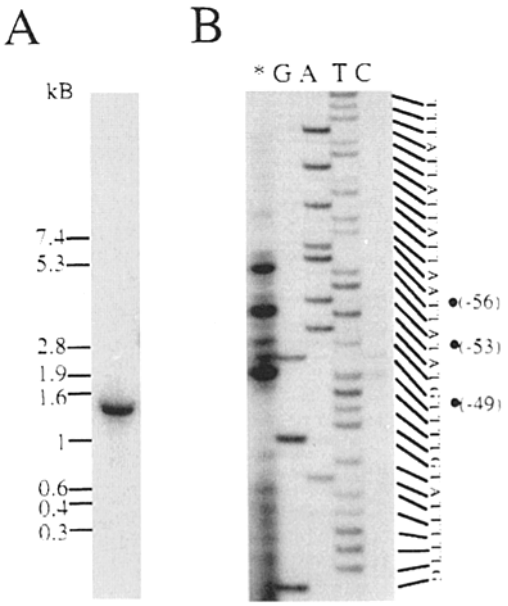

Figure 3. Transcript analysis. (*A*) Northern blot of total RNA isolated from wild type (CU428.1), probed with *GRL1* cDNA as described in Materials and Methods, and detected using a Phosphorimager. (*B*) Mapping of the 5′ end of the *GRL1* transcript. The asterisk marks the lane containing products of a primer extension reaction, as described in Materials and Methods. The adjacent four lanes contain products of a sequencing reaction on cloned *GRL1* using the same primer. The three major bands, at positions −56, −53, and −49 relative to the start codon, are indicated at the right.

the 5′ end of the mature transcript, primer extension was used to map the start sites to positions −49, −53, and −56, relative to the translation start site (Fig. 3 *B*). Such clusters of start sites have been observed for other *Tetrahymena* genes (70). Results of Southern blotting analysis using a *GRL1* probe against genomic DNA were also consistent with a single macronuclear gene copy (Fig. 4 *B*).

Targeted Disruption of GRL1

We transformed wild-type cells with the construct shown in Fig. 4 *A*, which contains a copy of the neomycin-resistance gene in an independent transcription unit, replacing bases −15 to +260 of *GRL1*. Transformation with this vector should lead initially to disruption of one or more macronuclear copies of the *GRL1* gene via homologous recombination (34). Growth of transformed clones in increasing concentrations of paromomycin resulted in selection of cells with progressively increasing replacement of *GRL1* by *GRL1:NEO2* copies, through a process called phenotypic assortment (13). After ~50 generations, Southern blotting analysis suggested that all endogenous macromolecular copies of *GRL1* had been replaced by the allele containing the disruption cassette (Fig. 4 *B*). The residual faint band probably corresponds to the intact micronuclear copy of *GRL1*, which is transcriptionally silent. Southern blotting analysis with a probe derived from *NEO2* demonstrated that recombination had occurred only within the endogenous *GRL1* locus (not shown). Most importantly, no Grl1p accumulation was detected by Western blotting analysis of whole cell lysates, which would have detected <1% of normal protein levels (Fig. 4 *C*). A second disruption strategy was also used, in which the *NEO2* casette was inserted at the EcoNI site. The results were identical. At least two independent clones were tested for each experiment, to assure that the results were not the consequence of unrelated secondary mutations induced during transformation. These *GRL1::NEO2* cells had no detectable defects except for those related to granule biosynthesis, described below.

Granule Morphogenesis in the Absence of Grl1p

The distribution of dense-core granules in wild-type *Tetrahymena* is highly characteristic and can be visualized using an mAb against a second identified granule protein, p80 (86). The p80 immunofluorescence pattern of *GRL1::NEO2* cells appeared identical to that of wild-type cells (Fig. 5 *A*, *first row*). Since this precise wild-type pattern of granule localization reflects the processes of granule synthesis, targeting, and docking, we infer that all three of these processes persist in the cells lacking Grl1p. The pattern also suggested that p80 accumulated only in a granule compartment, in the presence or absence of Grl1p. For further support, we sedimented postnuclear supernatants

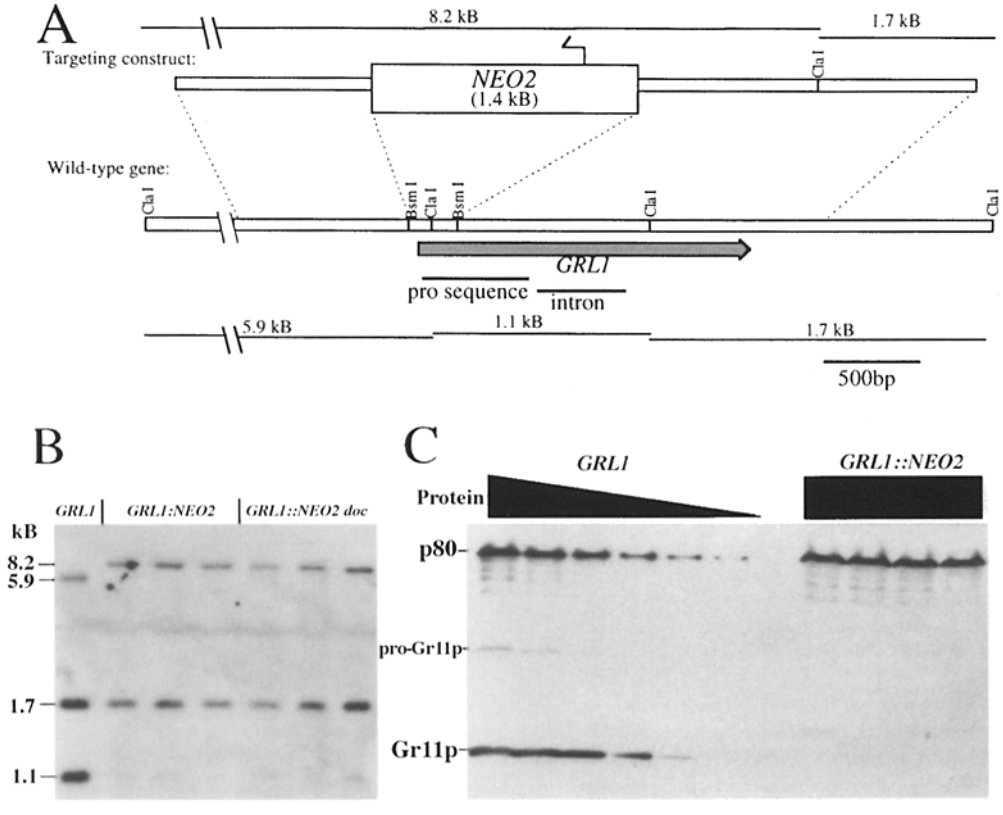

Figure 4. Genomic structure of the *T. thermophila GRL1* gene and Grl1p expression in control and transformed cells. (*A*) The gene conferring neomycin (and paromomycin) resistance, inserted between the histone H4 promoter region and the β-tubulin 3′ region (34), was inserted into the 5′ end of a genomic clone of *GRL1* as shown. The orientation of the *NEO* gene is indicated by an arrow. (*B*) Genomic DNA was prepared from *GRL1*, *GRL1::NEO2*, and *GRL1::NEO2* doc⁻ and digested with ClaI. Southern blotting using *GRL1* cDNA as probe was performed as described in Materials and Methods. Successful targeting resulted in elimination of the bands at 1.1 and 5.9 kb, concurrent with the appearance of a band at 8.2 kb. (*C*) Western blot analysis of transformants. *GRL1* and *GRL1::NEO2* cells (four independent transformants) were washed once and resuspended in 10 mM Hepes, pH 7. Whole cell lysates were prepared containing 1% SDS and 1 mM DTT, and protein concentrations were determined to permit equal loading for SDS-PAGE. 60 μg total protein was loaded for *GRL1::NEO2* samples and for a single sample of *GRL1* cells. In addition, dilutions of the wild-type sample containing 30, 15, 12.5, 3, and 1 μg total protein, were loaded in the successive adjacent lanes. After electrophoresis, samples were transferred to nitrocellulose and separately blotted with polyclonal antisera recognizing Grl1p and p80 and then visualized using ECL. Film was exposed for roughly 20 s. At longer exposures, a signal for Grl1p could also be detected for the lane corresponding to 1 μg of *GRL1* lysate, but not in *GRL1::NEO2* lanes.

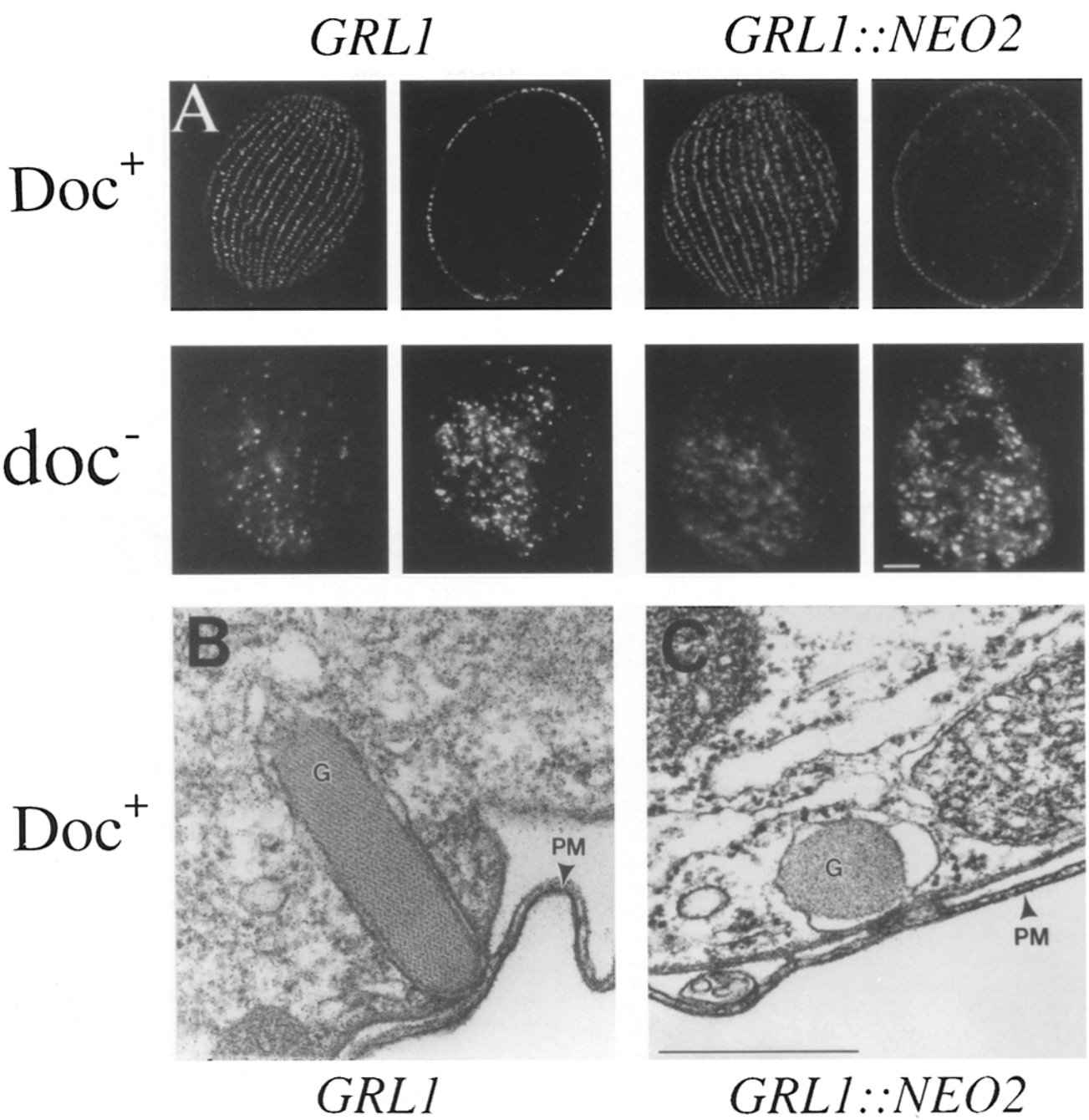

Figure 5. Appearance of secretory granules in *GRL1* and *GRL1::NEO2* cells, in both the CU428.1 (wild-type Doc$^+$) and MN173 (mutant doc$^-$) backgrounds. (*A*) Indirect immunofluorescence. Cells were fixed and visualized by indirect immunofluorescence using an mAb recognizing the granule protein p80. Each pair shows two views of the same cell, focusing on tangential and sagittal sections. In the Doc$^+$ background, both *GRL1* and *GRL1::NEO2* cells show similar patterns of punctate cortical immunofluorescence, corresponding to docked granules. In the doc$^-$ background, both *GRL1* and *GRL1::NEO2* show little surface immunofluorescence but substantial punctate cytoplasmic immunofluorescence, corresponding to nondocked granules. (*B*) Thin section of docked granule in Doc$^+$ *GRL1*. *G*, granule; *PM*, plasma membrane. (*C*) Thin section of docked granule in Doc$^+$ *GRL1::NEO2*. Granules lacking Grl1p are smaller, rounder, and do not contain a visible ordered matrix. Bars: (*A*) 10 μm; (*B* and *C*) 500 μm.

of *GRL1* and *GRL1::NEO2* lysates on Nycodenz gradients and compared the distributions of p80 by Western blotting analysis of gradient fractions. The distributions were superimposable and represented by a single peak (not shown). Thus, the absence of Grl1p does not result in detectable missorting of p80 to a nongranule compartment or the accumulation of a granule population with altered density. This is in contrast with other characterized mutants in granule morphogenesis, which accumulate presumed granule intermediates of a buoyant density less than that of the wild-type mature granules (87, and Turkewitz, A.P., unpublished).

Although properly positioned, the docked granules present in the *GRL1::NEO2* cells were morphologically aberrant. Wild-type granule cores have a characteristic rod shape, with typical dimensions along the long and short axes of 0.90 ± 0.1 and 0.19 ± 0.02 μm (n = 9) (Fig. 5 *B*). Granule cores lacking Grl1p resembled slightly deformed spheres with well-defined borders and had respective dimensions of 0.33 ± 0.02 and 0.27 ± 0.02 μm (n = 33) (Fig. 5 *C*). As in wild-type granules, the cores were highly condensed, and in many cases they did not fill the vesicle lumen. A notable difference in the organization of wild-type and mutant granule contents could be seen in electron microscope thin sections. Granules in wild-type cells contain an ordered protein lattice (Fig. 5 *B*) (43, 81). This could be seen even more clearly in purified granules that were negatively stained (see Fig. 7 *C*). In contrast, no lattices were ever seen in the spherical granules of *GRL1::NEO2* cells in thin sections (Fig. 5 *C*). Similarly, isolated spherical granules showed no internal lattice by negative staining (not shown).

Effect of GRL1 Disruption on Granule Function

When wild-type cells were stimulated with alcian blue, granule discharge resulted in formation within seconds of a thick flocculent coat surrounding the cells, composed of the released granule proteins (Fig. 6 *A*). Such rapid release is driven by the expansion of the granule lattice, which is thereby mechanically ejected from the cell (43). By optical microscopy, this protein coat has the appearance of a capsule in which the swimming cells are entrapped (12). In wild-type cultures, >95% of cells become encapsulated (80). When *GRL1::NEO2* cells were treated in an identical fashion, no capsules were formed, indicating that the absence of Grl1p led to a defect in regulated secretion (not shown). This defect was also observed using a second secretagogue, dibucaine (not shown). The basis for this defect was investigated by electron microscopy. Thin sections prepared from cells fixed shortly after stimulation revealed that the spherical granules underwent fusion with the plasma membrane upon stimulation, but that release of the core proteins was clearly different from that of wild-type granules. No thick flocculent coat was present, but instead small clumps of loosely linked fibers were frequently seen surrounding cells (Fig. 6, *B–D*). A second feature of the stimulated mutant cells was the persistence of unreleased granule protein. Whereas lattice expansion drives the rapid extrusion of granule contents in wild-type cells, in the *GRL1::NEO2* cells a remnant of the granule core was frequently still visible within the profiles of fused vesicles (Fig. 6, *B* and *C*). This material appeared less electron dense relative to cores of unstimulated docked granules. This suggests that while some expansion of the granule contents had occurred, either its extent or its coordination was inadequate for normal secretion. Therefore, the secretory defect arising from disruption of *GRL1* can be explained by a change in the pattern and/or timing of protein release from dense core granules.

Effect of GRL1 Disruption on Granule Composition

To determine the degree to which granule defects in *GRL1::NEO2* cells could be attributed to the absence of Grl1p, we compared wild-type and mutant granules to see

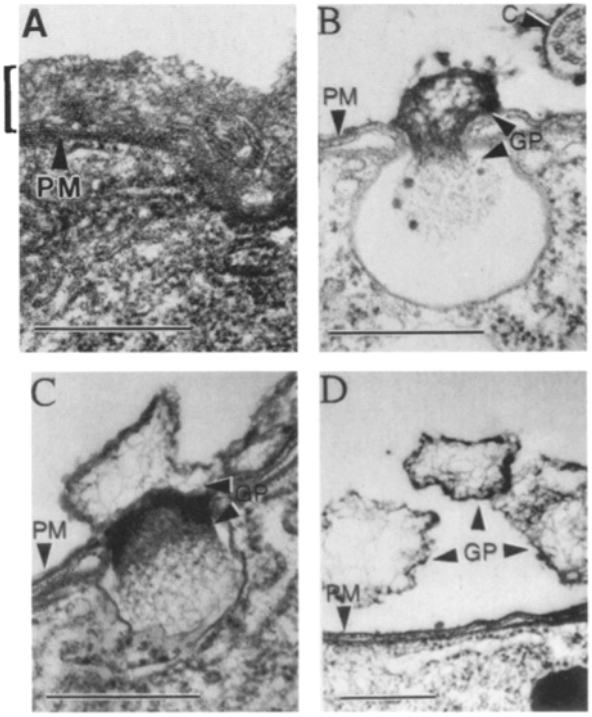

Figure 6. Granule exocytosis in wild-type and mutant cells. Cells were starved, stimulated with alcian blue, and fixed for electron microscopy after ~3 s, as described in Materials and Methods. (*A*) Doc$^+$ *GRL1* cells. A thick flocculent protein coat (indicated by a bracket) surrounding wild-type cells is formed by the rapid expansion and complete extrusion of granule lattices following exocytosis. (*B–D*) Doc$^+$ *GRL1::NEO2* cells. No flocculent coat is formed upon stimulation. Partial extrusion of granule cores is seen in *B* and *C*. The granule protein that is released, as illustrated in *D*, does not form a flocculent layer. Fibrillar elements can be seen within the secreted protein aggregates in *B–D*. The difference in appearance between the external and internal granule protein may be due to the differential accessibility to alcian blue. *C*, cilia; *PM*, plasma membrane; *GP*, granule protein.

whether the single gene disruption had pleiotropic effects on granule composition. Granules had previously been prepared from wild-type cells (87), but the yield was limited by the attachment of most granules to plasma membrane docking sites. This problem was now circumvented by using strain doc$^-$, one of a group of mutants that were recently selected based on the lack of a regulated exocytic response (Patterson, B., T. Soelter, E. Cole and A.P. Turkewitz, manuscript in preparation). In doc$^-$, granules accumulate in the cytoplasm rather than at the plasma membrane (Fig. 5 *A*, *second row*). Evidence that the defect does not reside in the granules themselves was provided by experiments in which doc$^-$ cells were observed shortly after conjugation with wild type, when limited cytoplasmic mixing occurs (56). Under these conditions, dramatic phenotypic reversal occurred as the entire set of cytoplasmic granules was rapidly recruited to the normal membrane docking sites (Melia, S.M., and A.P. Turkewitz, unpublished results). Phenotypically similar mutants in *Paramecium* have been described (6, 9).

A highly enriched granule fraction was prepared from doc$^-$ homogenates (Fig. 7 *B*). The granule protein lattice was clearly visible by negative staining of isolated granules

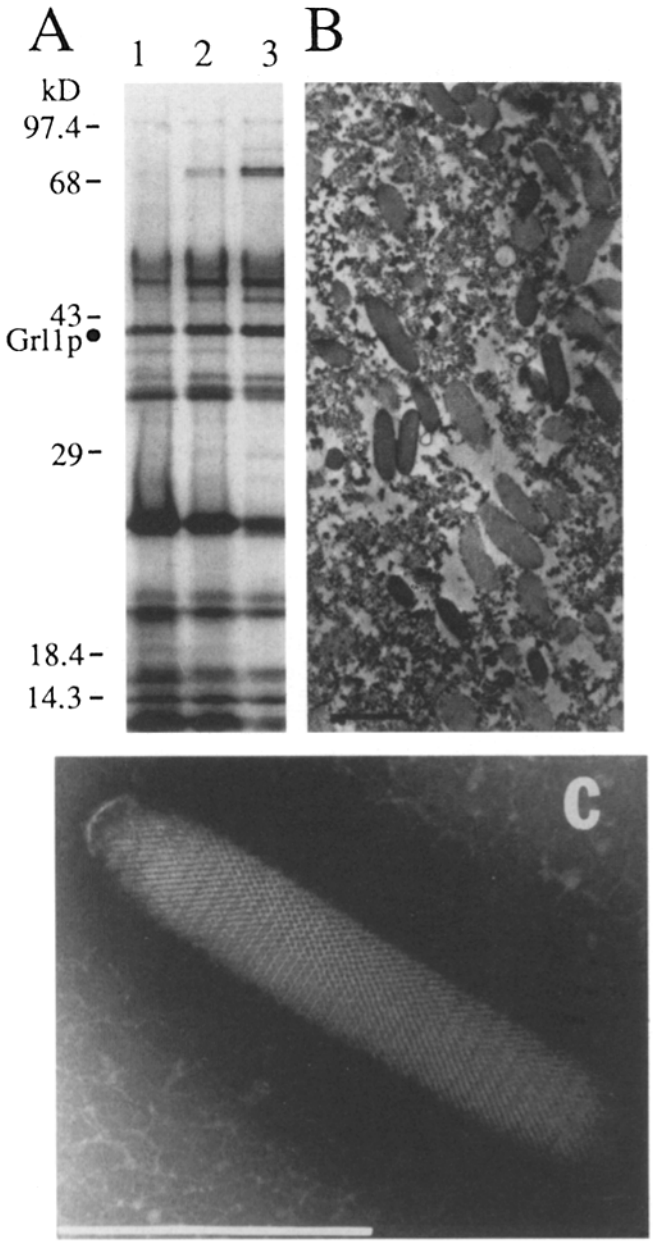

Figure 7. Analysis of isolated secretory granules. (*A*) SDS-PAGE of granule proteins, visualized with Coomassie blue. A nearly identical set of proteins are found in granules (prepared as described in Materials and Methods) and in purified secreted protein. Lanes *1* and *2*, two independent preparations of granules isolated from doc$^-$, 60 μg protein/lane; lane *3*, purified secreted protein from Doc$^+$, 60 μg protein. (*B*) Thin section electron micrograph of enriched granule preparation from doc$^-$ cells. (*C*) Negatively stained isolated granule from doc$^-$. A regular protein lattice is visible. Bars: (*B* and *C*) 500 nm.

(Fig. 7 *C*). We compared by SDS-PAGE the protein profile of this fraction to that of secreted granule proteins from wild-type cells (Fig. 7 *A*, lanes *1* and *2* vs *3*). Major proteins in the two fractions appeared identical. We note that since the secreted granule fraction was isolated as a large multimolecular complex, the correspondence between stored and released species strongly suggests that all major granule proteins remained coassociated after exocytosis.

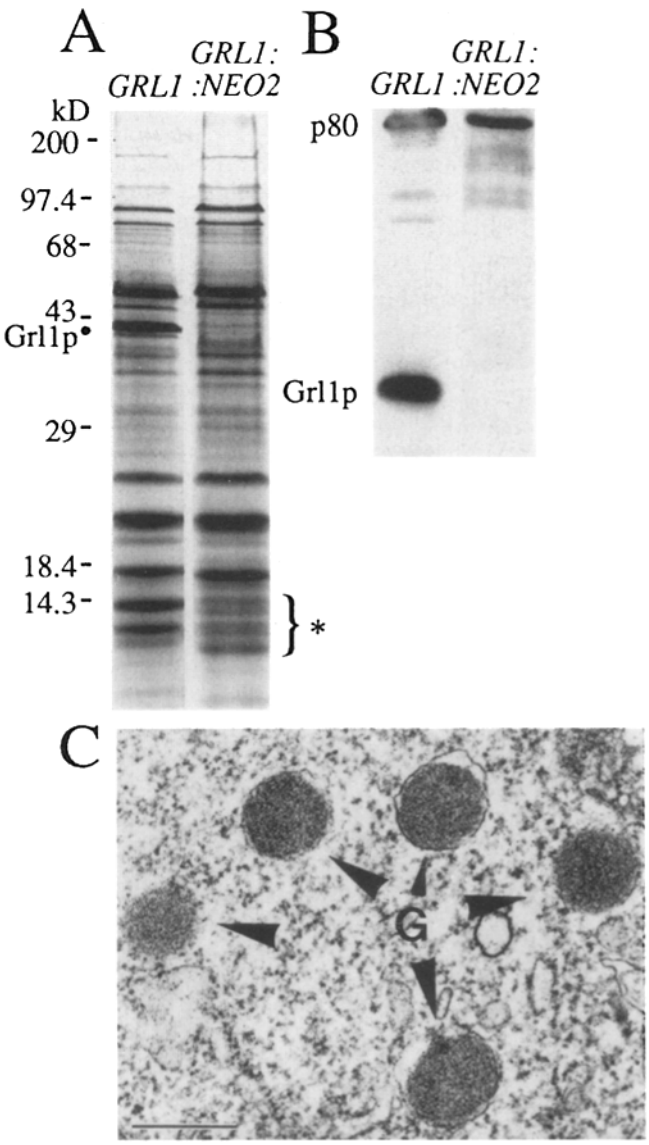

Figure 8. Comparison of protein content of granules from doc$^-$ and *GRL1::NEO2* doc$^-$. (*A*) Granules from *GRL1* doc$^-$ and *GRL1::NEO2* doc$^-$ cells were isolated and assayed for protein content. Aliquots containing 80 μg protein were electrophoresed on a 17.5% polyacrylamide gel, which was subsequently stained with Coomassie blue. Grl1p is indicated in the wild-type lane, and an asterisk marks a set of polypeptides that differ in the two samples. (*B*) Western blot analysis of enriched granule preparations from *GRL1* doc$^-$ and *GRL1::NEO2* doc$^-$. Aliquots containing 10 μg protein were electrophoresed on a 12.5% polyacrylamide gel and Western blotted with polyclonal antisera against Grl1p and p80. Bound antibodies were visualized using ECL. Film was exposed for ~5 s; no Grl1p signal appeared in the *GRL1::NEO2* lane at longer exposures. (*C*) Thin section electron micrograph of *GRL1::NEO2* doc$^-$, showing the cytoplasmic accumulation of undocked granules with no visible lattices. Bar, 500 nm.

To determine the composition of granules from cells lacking Grl1p, we created the double mutant *GRL1::NEO2* doc$^-$ by transforming doc$^-$ cells with the disruption cassette shown in Fig. 4 *A*. As described for transformation of wild-type cells, we obtained several clonal lines with no detectible intact *GRL1* macronuclear alleles (Fig. 4 *B*) or

protein (not shown). Immunofluorescence suggested that undocked granules were located in the cytoplasm (Fig. 5 *A*, *second row*), and electron microscopy of cell thin sections confirmed that these had the same spherical appearance as granules in *GRL1::NEO2* cells (Fig. 8 *C*). The *GRL1::NEO2* doc$^-$ granules were gradient purified and the absence of Grl1p confirmed by protein staining as well as Western blotting analysis (Fig. 8, *A* and *B*). The gross composition was compared to that of the parallel fraction prepared from doc$^-$, whose wild-type granules contain Grl1p (Fig. 8 *A*). Strikingly, nearly all of the other characteristic granule proteins were present at a relative abundance similar to those in wild-type granules. The exception was a difference between the wild-type and mutant granules in the cluster of low-M_r proteins (Fig. 8 *A*, *asterisk*). The mutant granules contained protein bands of similar, but not identical, mobility. These differences may reflect changes in granule-specific proteolytic cleavage, or alternatively may result from Grl1p-dependent sorting defects (see below). Differences in several minor bands were not consistent between preparations.

Discussion

The highly regular geometry of granule cores in wild-type cells reflects the orchestration of a set of proteins through a defined assembly program. It is easy to imagine that mutation or deletion of individual proteins in the ensemble could disrupt this process to various degrees, and granule maturation mutants that have been previously characterized in *Paramecium* (2) and *Tetrahymena* (87) may possibly involve defects in core proteins. Compared with these previously described cases, the *GRL1::NEO2* mutation is novel in two ways. First, it represents a defect in granule assembly for which the precise genetic lesion is defined. Secondly, this lesion appears to block completely the process of lattice formation without blocking granule accumulation, distinct from any previously characterized mutant strains. These include ten mutants in *Paramecium* (1, 70a) and six in *Tetrahymena* (Turkewitz, A.P., unpublished) that are marked by abnormal granule morphologies and/or partially ordered cores. However, it cannot be assumed that these mutants involve core proteins directly, since lattice assembly is implicitly dependent upon upstream steps in the secretory pathway.

A comparison between the pathways leading to granule exocytosis in wild-type and *GRL1* cells is presented in Fig. 9. Granules lacking Grl1p, although containing no identifiable lattice, nevertheless have uniformly condensed cores with well-defined edges. This appearance is distinct from that of immature granules in wild-type cells, in which a more disperse aggregate fills the entire vesicle space (36). Protein condensation in granules lacking Grl1p is likely to proceed during maturation via local protein interactions that define a first level of granule organization and that are established independently of Grl1p-dependent lattice formation. Such local organization of granule proteins in the mutant granules is also suggested by the presence of sparse fibrillar elements in images of the expanded cores of *GRL1::NEO2* cells, which indicate that some polymer formation has occurred. These fibrils resemble subunits of the much denser meshwork of secreted granule cores from wild-type cells (42).

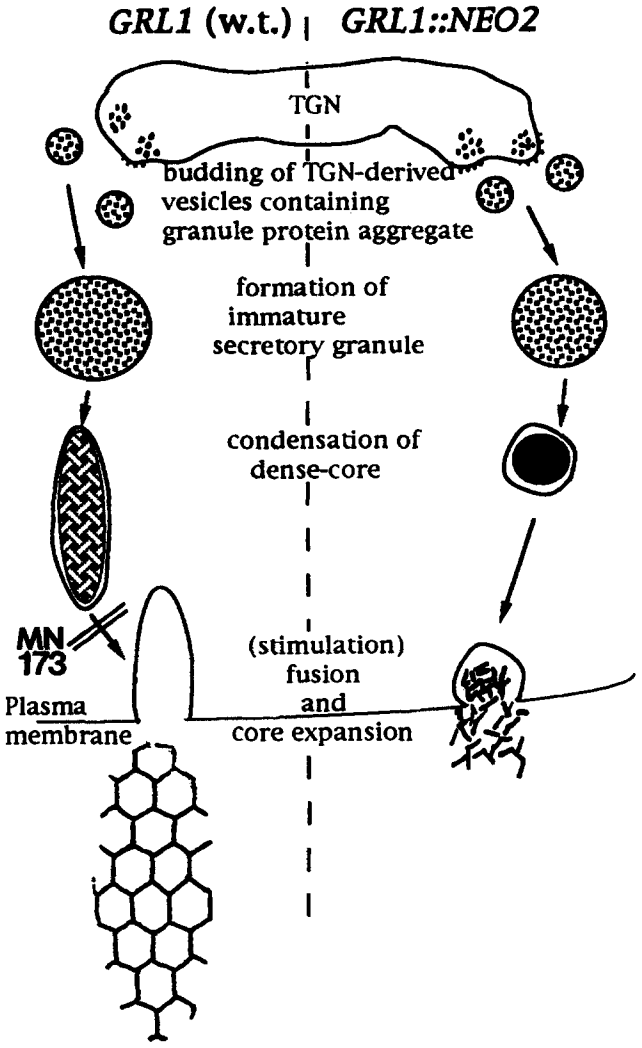

Figure 9. Model of the dense-core granule secretory pathway. Key features of four successive stages are compared in wild-type (*GRL1* Doc$^+$) and *GRL1::NEO2* Doc$^+$ cells: (*1*) The protein aggregation/sorting and vesicle budding steps that lead to formation of immature secretory granules occur in both wild-type and mutant cells. (*2*) Subsequent protein condensation during granule maturation occurs in the presence or absence of Grl1p, resulting in a dense core. However, in the absence of Grl1p, these cores are reduced in size and altered in shape. (*3*) Only in the presence of Grl1p is the core organized as a visible crystalline lattice. Mature granules are transported to and dock at the plasma membrane. This step is blocked in the MN173 doc$^-$ mutant. Upon stimulation, granule membranes fuse with the plasma membrane. (*4*) In wild-type granules, the core is extruded as the lattice rapidly expands to form an extended fibrous structure. *GRL1::NEO2* cells show much more modest protein secretion because of incomplete extrusion of granule cores resulting from their limited expansion.

The appearance of short- but not long-range organization in granules in *GRL1::NEO2* cells suggests that Grl1p plays a specific role in lattice assembly. This role may involve a structural transition related to proprotein processing (2), as previously suggested by the finding that processing of pro-Grl1p correlates with a change in the physical

state of the protein, from soluble to insoluble (87). We do not yet know with what other proteins Grl1p interacts in the granule. If the protein lattice is built on multivalent interactions, a number of other granule constituents may also be essential to establish the characteristic architecture. One must then assume that none of the genes for such proteins is affected within the pool of *Tetrahymena* or *Paramecium* exocytosis mutants derived by chemical mutagenesis, since no comparable phenotypes have been observed. This issue can be addressed by targeted disruption of other *Tetrahymena* granule protein genes.

Grl1p is essential for normal granule function, as shown by the limited postexocytic decondensation of granule cores in *GRL1::NEO2* cells. This may be explained as an indirect result of the failure to assemble a lattice, given that crystalloid granules have evolved in numerous ciliates as expandible mechanical devices involved in explosive protein secretion (43). However, preliminary results discussed below suggest that Grl1p may play an active role in expansion. The various changes observed in granules of *GRL1::NEO2* cells cannot be due to gross missorting of proteins since most of the other wild-type granule components are present. The exceptions are several polypeptides that appear changed in granules from *GRL1::NEO2* cells, that could therefore also affect granule organization. It is noteworthy that these differences are restricted to the smallest identifiable granule proteins (<14 kD), which therefore appear likely to be proteolytic products. Preliminary results suggest that the major polypeptide that appears to be absent in *GRL1::NEO2* granules is disulfide-linked to Grl1p in wild-type cells, and is likely to be derived from the Grl1p proregion. The appearance of a small unique polypeptide in *GRL1::NEO2* granules may be due to aberrant processing of other granule proteins that occurs in the absence of lattice assembly.

Normal processing to generate mature Grl1p occurs following lysine 188, and there is a roughly 16-residue basic region slightly amino-terminal to it. Similarly, in *Paramecium*, a block of basic amino acids is located slightly NH_2-terminal to an identified cleavage site within a tmp precursor, but no basic residues are found at the site itself (37, 53). The proximity of these basic regions to the cleavage sites is suggestive, since prohormone convertases in endocrine granules recognize dibasic and possibly monobasic targets (7, 8, 28). If the ciliate processing enzymes are related to characterized endocrine prohormone convertases, they are likely to be regulated quite differently. In endocrine granules, low pH and high calcium are important in regulating convertase activity (26). In contrast, granules in *Paramecium* do not appear to be acidified (36, 52a) and contain little calcium (10, 74).

Indeed, cytoplasmic granules may need to be actively maintained at low calcium concentrations, since calcium from the extracellular milieu can trigger granule decondensation after exocytosis (10). The targets for calcium binding and mechanism of expansion are unknown. However, calcium binds to Grl1p in vitro, and recent data suggest that this triggers an irreversible conformational transition (Turkewitz, A.P., manuscript in preparation). Thus, calcium binding to Grl1p in wild-type granules may be an important step in lattice expansion, which is similarly an irreversible process.

Homology searches of the protein database using the *GRL1* sequence identified a *Paramecium* dense-core granule lattice protein, T2-c, as well as other proteins with known coiled-coil structures, e.g., myosins. T2-c belongs to the tmp family of granule proteins in *Paramecium*, which are synthesized as precursors encoded by a large number of closely related genes (53). *GRL1* does not appear to belong to a gene family, based on DNA and RNA hybridization. In addition, several polyclonal anti-Grl1p antisera did not cross-react with other granule proteins (Turkewitz, A.P., unpublished observations). The sequence similarity to *Paramecium* TC-2 is too weak to provide firm evidence for evolutionary relatedness between Grl1p and tmps, but we note that diversity among ciliates is enormous; the genetic distance between the two organisms is similar to that between animals and plants (67). Nontheless, physicochemical similarities may suggest similar roles for Grl1p and tmps in formation of extensible lattices. Tmp precursors are roughly the same size as pro-Grl1p and are similarly hydrophilic and α-helical (37). A folded structure for tmp precursors has been proposed based on sequence analysis. It consists of two bundles of four-stranded antiparallel helices in which each short helix is identified by its heptad repeat motifs (37). Such motifs are also a feature of the predicted Grl1p sequence, leading us to compare the distribution of heptads with those in tmps. The introduction of a single 28-residue gap in the Grl1p sequence allowed close alignment of four heptad-defined regions with those in tmps, over a total length of 120 residues. This alignment also brings into near register the basic regions of the proteins, which may be functionally related as targets for recognition by converting enzymes. This comparison suggests structural similarity between amino-terminal domains of granule protein precursors in *Paramecium* and *Tetrahymena*.

Analysis of the carboxy-terminal halves of the proteins, however, was less conclusive. Again, Grl1p is strongly predicted to form coiled coils, but only by the introduction of multiple gaps in all sequences could we align heptads (not shown). There is also a significant difference between Grl1p and tmps in the ratio of charged to apolar residues, which in some cases may be diagnostic of short vs. extended helix formation. For three tmps, the ratios are 0.55, 0.73, and 0.74 respectively (37). That ratio for the proregion of Grl1p is 0.75, but for mature Grl1p it is 1.16, a ratio similar to that of extended α-fibrous proteins (25). The position of the intron at the boundary between the proregion and the mature protein may suggest an origin for Grl1p as a fusion between a tmp-like protein, now represented in the proregion, and a more extended α-helical protein.

Specific sorting of granule proteins is believed to depend upon aggregation intermediates in the TGN. One way to assess the interactions within these aggregates is to ask how well-defined perturbations might change the composition of the sorted product. This study showed the deletion of a single protein constituting 16% of normal granule content appeared to have relatively minor effects on the allocation of other granule proteins but a dramatic effect on granule function. We infer that the set of protein interactions involved in sorting and condensation is not identical to that present in the mature granule. Although Grl1p is a major lattice element, specific coassociation with Grl1p

does not appear to be an essential sorting step for granule proteins in general. If Grl1p in wild-type cells does play an important role in sorting/aggregation, that role must be compensated for by another core protein in the *GRL1::NEO2* cells. Several of the small (<25 kD) polypeptides in *Tetrahymena* DCGs are acidic and bind calcium in vitro and are thus candidates for such a role (Turkewitz, A.P., unpublished). None of these, however, appears to be overexpressed in the *GRL1::NEO2* cells.

Several models have been considered to account for sorting in the absence of specific heterotypic interactions: (*a*) Primary sorting could depend upon homoaggregation, with extensive reorganization in the maturing granule. This could account for the two distinct classes of immature granule vesicles seen in another ciliate, *Pseudomicrothorax* (64), and also appears consistent with formation of distinct classes of secretory granules in *Aplysia* neurons (31). (*b*) If the determinants for heterointeractions were common to multiple granule components, sorting would proceed in the absence of Grl1p based on equivalent interactions. (*c*) The majority of secretory protein traffic may be nonselectively directed to a post-TGN immature granule-like compartment, from which nongranule proteins would then be removed. This negative sorting could involve specific receptors or be the consequence of passive exclusion from a condensing core. This last model has been proposed for insulin-secreting cells and would appear efficient for such a system, in which granule proteins represent the bulk of secretory traffic (50). This issue has not been examined quantitatively in ciliates. Extension of the current approach in *Tetrahymena*, a biochemically and genetically manipulable system, should help to define individual vs. collective roles of proteins in the regulated secretory pathway.

We thank William Szechinski for technical assistance, John Perrino and Michael Lewis for EM, Paul Gardner for DNA sequencing, and Julie Feder for assistance with confocal microscopy. We gratefully acknowledge the help and advice of Alan Schwartz (Washington University) for protein sequencing, and of Steve Wickert for RNA isolation. Our thanks also go to Ted Steck, Adam Linstedt, Luisa Madeddu, Nava Segev, and Ben Glick for discussion and comments. For advice on transformation, we are indebted to Jacek Gaertig and to Jody Bowen and Martin Gorovsky. Conditions for biolistic transformation were developed by Peter Bruns and colleagues (D. Cassidy-Hanley, J. Bowen, J. Lee, E. Cole, L.A. VerPlank, J. Gaertig, M.A. Gorovsky, and P.J. Bruns, manuscript submitted for publication).

This work was supported by grants to A.P. Turkewitz from the National Institutes of Health (NIH; GM50946 and DK42086), the American Cancer Society (IRG-41-34), and the Cancer Research Foundation. N.D. Chilcoat was supported by an NIH predoctoral training grant GM07197, and A. Haddad was supported by predoctoral training grant GM071836.

Received for publication 9 August 1996 and in revised form 8 October 1996.

References

1. Adoutte, A. 1988. Exocytosis: biogenesis, transport and secretion of trichocysts. *In* Paramecium. H.D. Gortz, editor. Springer-Verlag, Berlin. 325–362.
2. Adoutte, A., N. Garreau de Loubresse, and J. Beisson. 1984. Proteolytic cleavage and maturation of the crystalline secretion products of *Paramecium*. *J. Mol. Biol.* 180:1065–1081.
3. Almers, W. 1990. Exocytosis. *Annu. Rev. Physiol.* 52:607–624.
4. Anderson, R.G.W., and L. Orci. 1988. A view of acidic intracellular compartments. *J. Cell Biol.* 106:539–543.
5. Attanoos, R.L., and A.K. Allen. 1987. The characterization of the proteins which are secreted by the mucocysts of *Tetrahymena thermophila*. *Biochim. Biophys. Acta.* 924:154–158.
6. Aufderheide, K.J. 1978. The effective sites of some mutations affecting exocytosis in *Paramecium tetraurelia*. *Mol. Gen. Genet.* 165:199–205.
7. Azaryan, A.V., T.J. Krieger, and V.Y. Hook. 1995. Purification and characteristics of the candidate prohormone processing proteases PC2 and PC1/3 from bovine adrenal medulla chromaffin granules. *J. Biol. Chem.* 270: 8201–8208.
8. Bailyes, E.M., K.I. Shennan, A.J. Seal, S.P. Smeekens, D.F. Steiner, J.C. Hutton, and K. Docherty. 1992. A member of the eukaryotic subtilisin family (PC3) has the enzymic properties of the type 1 proinsulin-converting endopeptidase. *Biochem. J.* 285:391–394.
9. Beisson, J., M. Lefort-Tran, M. Pouphile, M. Rossignol, and B. Satir. 1976. Genetic analysis of membrane differentiation in *Paramecium*: freeze-fracture study of the trichocyst cycle in wild-type and mutant strains. *J. Cell Biol.* 69:126–143.
10. Bilinski, M., H. Plattner, and H. Matt. 1981. Secretory protein decondensation as a distinct, Ca^{2+}-mediated event during the final steps of exocytosis in *Paramecium* cells. *J. Cell Biol.* 88:179–188.
11. Bonnemain, H., T. Gulik-Krzywicki, C. Grandchamp, and J. Cohen. 1992. Interactions between genes involved in exocytotic membrane fusion in *Paramecium*. *Genetics.* 130:461–470.
12. Bresslau, E. 1921. Die experimentalle Erzeugung von Hullen bei Infusorien als Parallele zur Membranbildung bei der kunstlichen Parthenogenese. *Naturwissenschaften.* 9:57–62.
13. Bruns, P.J. 1986. Genetic organization of *Tetrahymena*. *In* The Molecular Biology of Ciliated Protozoa. J. Gall, editor. Academic Press, New York. 27–44.
14. Bruns, P.J., and T.B. Brussard. 1974. Positive selection for mating with functional heterokaryons in *Tetrahymena pyriformis*. *Genetics.* 78:831–841.
15. Burgess, T.L., and R.B. Kelly. 1987. Constitutive and regulated secretion of proteins. *Annu. Rev. Cell Biol.* 3:243–293.
16. Burgoyne, R.D. 1991. Control of exocytosis in adrenal chromaffin cells. *Biochim. Biophys. Acta.* 1071:174–202.
17. Carnell, L., and H.-P.H. Moore. 1994. Transport via the regulated secretory pathway in semi-intact PC12 cells: role of intra-cisternal calcium and pH in the transport and sorting of secretogranin II. *J. Cell Biol.* 127:693–705.
18. Cathala, G., J.F. Savouret, B. Mendez, B.L. West, M. Karin, J.A. Martial, and J.D. Baxter. 1983. A method for the isolation of intact, translationally active ribonucleic acid. *DNA.* 2:329–335.
19. Chanat, E., and W.B. Huttner. 1991. Milieu-induced, selective aggregation of regulated secretory proteins in the *trans*-Golgi network. *J. Cell Biol.* 115:1505–1519.
20. Chandra, S., E.P.W. Kable, G.H. Morrison, and W.W. Webb. 1991. Calcium sequestration in the Golgi apparatus of cultured mammalian cells revealed by laser scanning confocal microscopy and ion microscopy. *J. Cell Sci.* 100:747–752.
21. Cole, E.S., and P.J. Bruns. 1993. Uniparental cytogamy: a novel, efficient method for bringing mutations of *Tetrahymena* into homozygous expression with precocious sexual maturity. *Genetics.* 132:1017–1031.
22. Cole, E.S., and K.R. Stuart. 1991. Biochemical and cytological evidence for an overabundance of mucocysts in the bcd pattern mutant of *Tetrahymena thermophila*. *J. Protozool.* 38:536–547.
23. Collins, T., and J.M. Wilhelm. 1981. Post-translational cleavage of mucocyst precursors in *Tetrahymena*. *J. Biol. Chem.* 256:10475–10484.
24. Colomer, V., G.A. Kicska, and M.J. Rindler. 1996. Secretory granule content proteins and the luminal domains of granule membrane proteins aggregate in vitro at mildly acidic pH . *J. Biol. Chem.* 271:48–55.
25. Conway, J.F., and D.A.D. Parry. 1990. Structural features in the heptad substructure and longer range repeats of two-stranded α-fibrous proteins. *Int. J. Biol. Macromol.* 12:328–334.
26. Davidson, H.W., C.J. Rhodes, and J.C. Hutton. 1988. Intraorganellar calcium and pH control proinsulin cleavage in the pancreatic β cell via two distinct site-specific endopeptidases. *Nature (Lond.).* 333:93–96.
27. Ding, Y., A. Ron, and B.H. Satir. 1991. A potential mucus precursor in Tetrahymena wild type and mutant cells. *J. Protozool.* 38:613–623.
28. Docherty, K., and D.F. Steiner. 1982. Post-translational proteolysis in polypeptide hormone biosynthesis. *Annu. Rev. Physiol.* 44:625–638.
29. Farquhar, M.G., and G.E. Palade. 1981. The Golgi apparatus (complex)-(1954-1981)-from artifact to center stage. *J. Cell Biol.* 91:77s–103s.
30. Farrell, R.E.J. (1993). RNA Methodologies: A Laboratory Guide for the Isolation and Characterization. Academic Press, New York. 126–204.
31. Fisher, J.M., W. Sossin, R. Newcomb, and R.H. Scheller. 1988. Multiple neuropeptides derived from a common precursor are differentially packaged and transported. *Cell.* 54:813–822.
32. Gaertig, J., and M.A. Gorovsky. 1992. Efficient mass transformation of *Tetrahymena thermophila* by electroporation of conjugants. *Proc. Natl. Acad. Sci. USA.* 89:9196–9200.
33. Gaertig, J., T.H. Thatcher, K.E. McGrath, R.C. Callahan, and M.A. Gorovsky. 1993. Perspectives on tubulin isotype function and evolution based on the observation that *Tetrahymena thermophila* microtubules contain a single alpha- and beta-tubulin. *Cell Motil. Cytoskel.* 25:243–253.
34. Gaertig, J., L. Gu, B. Hai, and M.A. Gorovsky. 1994. High frequency vector-mediated transformation and gene replacement in *Tetrahymena*. *Nucl. Acids Res.* 22:5391–5398.

35. Gaertig, J., T.H. Thatcher, and M.A. Gorovsky. 1995. Gene transfer by electroporation of *Tetrahymena*. *In* Electroporation Protocols for Microorganisms. J.A. Nickoloff, editor. Humana Press, Totawa, NJ. 331–348.
36. Garreau de Loubresse, N. 1993. Early steps of the secretory pathway in *Paramecium*. *In* Membrane Traffic in Protozoa. JAI Press, Greenwich, CT. 27–60.
36a. Garreau de Loubresse, N., M.-C. Gautier, and L. Sperling. 1994. Immature secretory granules are not acidic in *Paramecium*: implications for sorting to the regulated pathway. *Biol. Cell.* 82:139–147.
37. Gautier, M.-C., L. Sperling, and L. Madeddu. 1996. Cloning and sequence analysis of genes coding for *Paramecium* secretory granule (trichocyst) proteins. *J. Biol. Chem.* 271:10247–10255.
38. Gerdes, H.-H., P. Rosa, E. Phillips, P.A. Baeuerle, R. Frank, P. Argos, and W.B. Huttner. 1989. The primary structure of human secretogranin II, a widespread tyrosine-sulfated secretory granule protein that exhibits low pH - and calcium-induced aggregation. *J. Biol. Chem.* 264:12009–12015.
39. Gorr, S.-U., W.L. Dean, T.L. Radley, and D.V. Cohn. 1988. Calcium-binding and aggregation properties of parathyroid secretory protein-I (chromogranin A). *Bone Miner.* 4:17–25.
40. Gorr, S.-U., J. Shioi, and D.V. Cohn. 1989. Interaction of calcium with porcine adrenal chromogranin (secretory protein-I) and chromogranin B (secretogranin I). *Am. J. Physiol.* 257:E247–E254.
41. Gutierrez, J.C., and E. Orias. 1992. Genetic characterization of *Tetrahymena thermophila* mutants unable to secrete capsules. *Dev. Genet.* 13: 160–166.
42. Hausmann, K. 1972. Cytologische studien an Trichocysten. IV. - die Feinstruktur ruhender und ausgeschiedener Protrichocysten von *Loxophyllum*, *Tetrahymena*, *Prorodon* und *Lacrymaria*. *Protistologica.* 8:401–412.
43. Hausmann, K. 1978. Extrusive organelles in protists. *Int. Rev. Cytol.* 52: 197–276.
44. Hausmann, K., A.K. Fok, and R.D. Allen. 1988. Immunocytochemical analysis of trichocyst structure and development in *Paramecium*. *J. Ultrastruct. Mol. Struct. Res.* 99:213–225.
45. Horowitz, S., J.K. Bowen, G.A. Bannon, and M.A. Gorovsky. 1987. Unusual features of transcribed and translated regions of the histone H4 gene family of *Tetrahymena thermophila*. *Nucleic Acids Res.* 15:141–160.
46. Huttner, W.B., and S.A. Tooze. 1989. Biosynthetic protein transport in the secretory pathway. *Curr. Opin. Cell Biol.* 1:648–654.
47. Kahn, R.W., B.H. Andersen, and C.F. Brunk. 1993. Transformation of *Tetrahymena thermophila* by microinjection of a foreign gene. *Proc. Natl. Acad. Sci. USA.* 90:9295–9299.
48. Kelly, R.B. 1985. Pathways of protein secretion in eukaryotes. *Science (Wash. DC).* 230:25–32.
49. Kerboeuf, D., A. Le Berre, J.-C. Dedieu, and J. Cohen. 1993. Calmodulin is essential for assembling links necessary for exocytic membrane fusion in *Paramecium*. *EMBO (Eur. Mol. Biol. Organ.) J.* 12:3385–3390.
50. Kuliawat, R., and P. Arvan. 1992. Protein targeting via the "constitutive-like" secretory pathway in isolated pancreatic islets: passive sorting in the immature granule compartment. *J. Cell Biol.* 118:521–529.
51. Laemmli, U.K. 1970. Cleavage of structural proteins during assembly of the head of bacteriophage T4. *Nature (Lond.).* 227:680–682.
52. Lefort-Tran, M., K. Aufderheide, M. Pouphile, M. Rossignol, and J. Beisson. 1981. Control of exocytic processes: cytological, and physiological studies of trichocyst mutants in *Paramecium tetraurelia*. *J. Cell Biol.* 88: 301–311.
52a. Lumpert, C.J., R. Glas-Albrecht, E. Eisenmann, and H. Plattner. 1992. Secretory organelles in *Paramecium* cells (trichocysts) are not remarkably acidic compartments. *J. Histochem. Cytochem.* 40:153–160.
53. Madeddu, L., M.-C. Gautier, L. Vayssié, A. Houari, and L. Sperling. 1995. A large multigenic family codes for the polypeptides of the crystalline trichocyst matrix in *Paramecium*. *Mol. Biol. Cell.* 6:649–659.
54. Maihle, N.J., and B.H. Satir. 1986. Protein secretion in *Tetrahymena thermophila*. Characterization of the major proteinaceous secretory proteins. *J. Biol. Chem.* 261:7566–7570.
55. Martindale, D.W. 1989. Codon usage in *Tetrahymena*, and other ciliates. *J. Protozool.* 36:29–34.
56. McDonald, B.B. 1966. The exchange of RNA and protein during conjugation in *Tetrahymena*. *J. Protozool.* 13:277–285.
57. Miller, S.G., and H.P. Moore. 1990. Regulated secretion. *Curr. Opin. Cell Biol.* 2:642–647.
58. Ochman, H., A.S. Gerber, and D.L. Hartl. 1988. Genetic applications of an inverse polymerase chain reaction. *Genetics.* 120:621–623.
59. Orci, L., M. Ravazzola, and A. Perrelet. 1984. (Pro)insulin associates with Golgi membranes of pancreatic B cells. *Proc. Natl. Acad. Sci. USA.* 81: 6743–6746.
60. Orci, L., M. Ravazzola, M. Amherdt, O. Madsen, J.-D. Vassalli, and A. Perrelet. 1985. Direct identification of prohormone conversion site in insulin-secreting cells. *Cell.* 42:671–681.
61. Orci, L., M. Ravazzola, M. Amherdt, A. Perrelet, S.K. Powell, D.L. Quinn, and H.-P.H. Moore. 1987. The trans-most cisternae of the Golgi complex: a compartment for sorting of secretory, and plasma membrane proteins. *Cell.* 51:1039–1051.
62. Orci, L., M. Ravazzola, M.-J. Storch, R.G.W. Anderson, J.-D. Vassalli, and A. Perrelet. 1987. Proteolytic maturation of insulin is a post-Golgi event which occurs in acidifying clathrin-coated secretory vesicles. *Cell.* 49: 865–868.
63. Orias, E., M. Flacks, and B.H. Satir. 1983. Isolation and ultrastructural characterization of secretory mutants of *Tetrahymena thermophila*. *J. Cell Sci.* 64:49–67.
64. Peck, R.K., B. Swiderski, and A.-M. Tourmel. 1993. Involvement of the trans-Golgi network, coated vesicles, vesicle fusion, and secretory product condensation in the biogenesis of *Pseudomicrothorax* trichocysts. *In* Membrane Traffic in Protozoa. H. Plattner, editor. JAI Press, Greenwich, CT. 1–26.
65. Plattner, H., C.J. Lumpert, G. Knoll, R. Kissmehl, B. Hohne, M. Momayezi, and A.R. Glas. 1991. Stimulus-secretion coupling in *Paramecium* cells. *Eur. J. Cell Biol.* 55:3–16.
66. Pollack, S. 1974. Mutations affecting the trichocysts in *Paramecium aurelia*. I. Morphology and description of the mutants. *J. Protozool.* 21:352–362.
67. Prescott, D.M. 1994. The DNA of ciliated protozoa. *Microbiol. Rev.* 58: 233–267.
68. Proudfoot, N.J., and E. Whitelaw. 1988. Termination and 3' end processing of eukaryotic RNA. *In* Transcription and Splicing. B.D. Hames and B.M. Glover, editors. IRL Press, Oxford. 97.
69. Rindler, M.J. 1992. Biogenesis of storage granules and vesicles. *Curr. Opin. Cell Biol.* 4:616–622.
70. Rosendahl, G., P.H. Andreasen, and K. Kristiansen. 1991. Structure and evolution of the *Tetrahymena thermophila* gene encoding ribosomal protein L21. *Gene.* 98:161–167.
70a. Ruiz, F., A. Adoutte, M. Rossignol, and J. Beisson. 1976. Genetic analysis of morphogenetic processes in *Paramecium*. *Genet. Res.* 27:109–122.
71. Russell, J.T. 1987. The secretory vesicle in processing and secretion of neuropeptides. *Curr. Top. Membr. Transp.* 31:277–312.
72. Sambrook, J., E.J. Fritsch, and T. Maniatis. 1989. Molecular Cloning: A Laboratory Manual. CSH Lab Press, Plainview, NY.
72a. Sanford, J.C., F.D. Smith, and J.A. Russell. 1993. Optimizing the biolistic process for different biological applications. *Methods Enzymol.* 217: 283–509.
73. Satir, B.H., M. Reichman, and E. Orias. 1986. Conjugation rescue of an exocytosis-competent membrane microdomain in *Tetrahymena thermophila* mutants. *Proc. Natl. Acad. Sci. USA.* 83:8221–8225.
74. Schmitz, M., R. Meyer, and K. Zierold. 1985. X-ray microanalysis in cryosections of natively frozen *Paramecium caudatum* with regard to ion distribution in ciliates. *Scanning Electron Microsc.* 1:443–445.
75. Schuel, H. 1978. Secretory functions of egg cortical granules in fertilization and development: a critical review. *Gamete Res.* 1:299–382.
76. Shennan, K.I.J., N.A. Taylor, and K. Docherty. 1994. Calcium- and pH-dependent aggregation and membrane association of the precursor of the prohormone convertase PC2. *J. Biol. Chem.* 269:18646–18650.
77. Sherman, F. 1991. Getting started with yeast. *In* Guide to Yeast Genetics and Molecular Biology. C. Guthrie and G.R. Fink, editors. Academic Press, San Diego, CA. 3–20.
78. Steers, E., Jr., J. Beisson, and V.T. Marchesi. 1969. A structural protein extracted from the trichocysts of *Paramecium aurelia*. *Exp. Cell Res.* 57: 392–396.
79. Steiner, D.F. 1991. Prohormone convertases revealed at last. *Curr. Biol.* 1: 375–377.
80. Tiedtke, A. 1976. Capsule shedding in *Tetrahymena*. *Naturwissenschaften.* 63:93.
81. Tokuyasu, K., and O.H. Scherbaum. 1965. Ultrastructure of mucocysts and pellicle of *Tetrahymena pyriformis*. *J. Cell Biol.* 27:67–81.
82. Tooze, J., and S.A. Tooze. 1986. Clathrin-coated vesicular transport of secretory proteins during the formation of ACTH-containing secretory granules in AtT20 cells. *J. Cell Biol.* 103:839–850.
83. Tooze, J., H.F. Kern, S.D. Fuller, and K.E. Howell. 1989. Condensation-sorting events in the rough endoplasmic reticulum of exocrine pancreatic cells. *J. Cell Biol.* 109:35–50.
84. Tooze, S.A. 1991. Biogenesis of secretory granules. Implications arising from the immature secretory granule in the regulated pathway of secretion. *FEBS J.* 2:220–224.
85. Tooze, S.A., T. Flatmark, J. Tooze, and W.B. Huttner. 1991. Characterization of the immature secretory granule, an intermediate in granule biogenesis. *J. Cell Biol.* 115:1491–1503.
86. Turkewitz, A.P., and R.B. Kelly. 1992. Immunocytochemical analysis of secretion mutants of *Tetrahymena* using a mucocyst-specific monoclonal antibody. *Dev. Genet.* 13:151–159.
87. Turkewitz, A.P., L. Madeddu, and R.B. Kelly. 1991. Maturation of dense core granules in wild type and mutant *Tetrahymena thermophila*. *EMBO (Eur. Mol. Biol. Organ.) J.* 10:1979–1987.
88. Von Heijne, G. 1983. Patterns of amino acids near signal-sequence cleavage sites. *Eur. J. Biochem.* 133:17–21.
89. Winkler, H., and R. Fischer-Colbrie. 1992. The chromogranins A and B: the first 25 years and future perspectives. *Neuroscience.* 3:497–528.
90. Yoo, S.H., and J.P. Albanesi. 1990. Ca^{2+}-induced conformational change and aggregation of chromogranin A. *J. Biol. Chem.* 265:14414–14421.